Published in final edited form as:

Wiley Interdiscip Rev Syst Biol Med. 2018 September ; 10(5): e1421. doi:10.1002/wsbm.1421.

Systems Approaches to Optimizing Deep Brain Stimulation Therapies in Parkinson's Disease

Sabato Santaniello[1], **John T. Gale**[2], **Sridevi V. Sarma**[3]

Sabato Santaniello: sabato.santaniello@uconn.edu; John T. Gale: jtgale@emory.edu; Sridevi V. Sarma: sridevi.sarma@jhu.edu

[1]Biomedical Engineering Department and CT Institute for the Brain and Cognitive Sciences, University of Connecticut; ORCID-ID: 0000-0002-2133-9471

[2]Department of Neurosurgery, Emory University School of Medicine

[3]Department of Biomedical Engineering and Institute for Computational Medicine, Johns Hopkins University

Abstract

Over the last thirty years, deep brain stimulation (DBS) has been used to treat chronic neurological diseases like dystonia, obsessive-compulsive disorders, essential tremor, Parkinson's disease, and more recently, dementias, depression, cognitive disorders, and epilepsy. Despite its wide use, DBS presents numerous challenges for both clinicians and engineers. One challenge is the design of novel, more efficient DBS therapies, which are hampered by the lack of complete understanding about the cellular mechanisms of therapeutic DBS. Another challenge is the existence of redundancy in clinical outcomes, i.e., different DBS programs can result in similar clinical benefits but very little information (e.g., predictive models, longitudinal data, metrics, etc.) is available to select one program over another. Finally, there is high variability in patients' responses to DBS, which forces clinicians to carefully adjust the stimulation settings to each patient via lengthy programming sessions. Researchers in neural engineering and systems biology have been tackling these challenges over the past few years with the specific goal of developing novel DBS therapies, design methodologies, and computational tools that optimize the therapeutic effects of DBS in each patient. Furthermore, efforts are being made to automatically adapt the DBS treatment to the fluctuations of disease symptoms. A review of the quantitative approaches currently available for the treatment of Parkinson's disease is presented here with an emphasis on the contributions that systems theoretical approaches have provided to understand the global dynamics of complex neuronal circuits in the brain under DBS.

1. INTRODUCTION

Chronic deep brain stimulation (DBS) devices (Fig. 1) were first approved by the US Food and Drug Administration (FDA) in 1997 to treat tremor. Since then, DBS therapies have been used to treat patients with Parkinson's disease (PD), dystonia, obsessive-compulsive

DISCLOSURE

The authors declare no conflict of interest to be disclosed at the time of publication.

disorders, and epilepsy [1, 2]. More recent applications of DBS include the treatment of refractory depression, psychiatric disorders, and neurodegenerative dementias [3–5].

In patients with advanced PD, DBS is used to ameliorate motor symptoms and reduce motor fluctuations while decreasing the dosages of anti-parkinsonian medications [6, 7], which leads to a more efficient and prolonged management of the PD symptoms [1, 2]. Clinical ratings of motor symptoms typically improve by more than 50% in appropriately selected PD patients [1] and this explains the increasing number of patients (8,000–10,000) who receive DBS surgery every year compared to patients with other neurological diseases [8].

The success of DBS, though, critically depends on the parameters defining the electrical pulses delivered by the pulse generator (i.e., duration, amplitude, and frequency) and must be carefully assigned (Fig. 1) [9]. Tuning of the DBS parameters must account for the unique combination of symptoms that each patient presents and may require several adjustments [10]. Because of the therapeutic relevance of the stimulation parameters, current clinical protocols require that the DBS devices are programmed manually through multiple sessions over a few days or weeks. During these sessions, the range of viable parameter values must be carefully probed while a trained clinician (e.g., neurologist, neurosurgeon, fellow, occupational therapist, etc.) must evaluate the symptomatic benefits of the stimulation by using clinical rating scales and finally identify the most adequate parameter values [11].

The complexity and time-consuming nature of these programming protocols has promoted an intense research activity to devise new computational tools that may assist the clinicians and shorten the programming phase. In this effort, researchers in neural control and systems biology had an important role in pioneering closed-loop programming procedures, adaptive DBS solutions, and model-based control policies that may optimize the therapeutic effects of DBS while coping with the fluctuations of the disease symptoms. Moreover, computational models and systems analyses have been developed to investigate the cellular mechanisms of therapeutic DBS protocols and to design novel DBS technologies.

We provide here a review of the quantitative approaches that have been recently developed for the treatment of Parkinson’s disease via DBS, with an emphasis on the contributions that systems theoretical approaches have provided to understand the global dynamics of complex neuronal circuits in the brain under DBS. Several modeling approaches have been proposed to describe the brain dynamics under PD and to personalize the DBS therapy, e.g., see (Lowery, 2017) [12] for a comprehensive overview. Our goal here is to review the implications and insights that have been gained by using a systems theoretical approach in association with these models to analyze the neural dynamics and optimize the DBS therapy via model-based techniques.

2. BASAL GANGLIA AND PARKINSON’S DISEASE

Current protocols for DBS surgery in PD recommend the placement of the DBS electrode in either the subthalamic nucleus (STN) or the internal globus pallidus (GPi) [9, 13] in the basal ganglia (Fig. 1).

The basal ganglia are a group of subcortical nuclei involved in multiple segregated circuits (e.g., limbic, prefrontal, motor, oculomotor loop) that modulate the cortical activity [14] (Fig. 2a). The motor circuit is involved in the planning of movements and consists of multiple parallel polysynaptic loops, which are hypothesized to convey bits of information (independent of the other loops) about a selected motor program [15, 16]. Each loop in the motor circuit begins with a convergent input from the premotor and sensorimotor cortices to the striatum (putamen region, [17]) and then proceeds through different pathways to the GPi or the substantia nigra pars reticularis (SNr), which project to the ventrolateral thalamus and the brainstem. The ventrolateral thalamus is believed to process, integrate, and relay sensory information selectively to the sensorimotor, premotor, and motor cortices [14, 18]. Other nuclei involved in the motor circuit are the substantia nigra pars compacta (SNc), the STN, and the external globus pallidus (GPe). A widely accepted functional model [19] suggests that there are two dopamine-mediated pathways through the BG motor circuit (i.e., the direct and indirect pathway, see Fig. 2a). Based on the polarities of known connections, the direct pathway is thought to facilitate movements while the indirect pathway is thought to suppress movements.

Parkinson's disease degenerates the neurons in the SNc and the consequent loss of dopamine alters the function of these pathways [15] (Fig. 2b) and contributes to the emergence of the movement disorders. A functional explanation for the effects of dopamine depletion on the basal ganglia was first provided by Albin and DeLong in the model [19]. Based on anatomical and physiological considerations, they observed that there are different types of dopaminergic receptors in the putamen, i.e., D_1-type for the direct pathways and D_2-type for the indirect pathways, respectively, which have opposite effects on the activation of the striatal neurons [20]. Specifically, a loss of dopamine would suppress the striatal neurons projecting onto the GPi and therefore inhibit the direct pathway. Conversely, a loss of dopamine would facilitate the activity of the neurons projecting onto the GPe, thus exciting the indirect pathway (Fig. 2b). A result of this dual effect would be an over-inhibition of the thalamus, which would corrupt the information relayed back to cortex [14, 19].

It is important to note that such arguments were originally phrased in terms of average firing rates of neurons. Numerous experimental studies later demonstrated that the dynamics, i.e., the temporal arrangement of the spikes, in the basal ganglia neurons play an important role in the pathophysiology of Parkinson's disease. First, it has been shown that a severe deficiency of dopamine positively correlates with the formation of abnormal oscillatory activity, mostly confined to the beta band (13–35 Hz), throughout the entire system of the basal ganglia [21–29]. These oscillations are suppressed by medications that target the central dopaminergic activity and their amplitude correlates with the intensity of the bradykinesia and rigidity symptoms of PD [27, 30]. Furthermore, the beta activity is phasic and organized in long, high-amplitude bursts [31], which suggests a pervasive oscillatory synchronization within the entire motor circuit.

Second, studies [32, 33] quantified the ability of the neurons in the ventrolateral thalamus to encode sensorimotor information such as tactile stimuli and passive movements of the limbs under PD conditions. They reported that the selectivity of the thalamic response to

the stimuli significantly decreases under dopamine depletion, which may indicate a loss of functional segregation along the loops forming the motor circuit.

Overall, there is converging evidence suggesting that, under Parkinsonian conditions, the parallel loops forming the motor circuit become rhythmic and overly-synchronized, which consequently limits their ability to convey independent bits of information about specific motor programs through different, parallel pathways [15].

3. DBS THERAPY

The DBS implant consists of an electrode lead inserted in the basal ganglia (STN or GPi) and connected to an insulated wire (a.k.a. “extension”) that passes under the skin of the head, neck and shoulder and terminates at the implanted pulse generator (Fig. 1). The pulse generator sits inferior to the collar bone and delivers electrical stimulation to the tip of the electrode via the extension.

The generator delivers voltage-controlled, charge-balanced pulses with a regular pattern (i.e., constant inter-pulse intervals) and the typical parameter settings of voltage, pulse width, and frequency range from 1–3.5 V, 60–210 μs, and 130–185 Hz, respectively [34–36]. In a large, multi-center study involving PD patients [37], Obeso and colleagues determined the mean stimulus parameter settings being 3 V, 82 μs, and 152 Hz for STN DBS, and 3.2 V, 125 μs, and 162 Hz for GPi DBS, respectively.

The ranges of voltage, pulse width, and frequency were mainly determined through empirical studies conducted on relatively homogenous groups of PD patients. For instance, Rizzoni and colleagues [36] estimated the relationship between pulse width and stimulus intensity (i.e., voltage) while monitoring the patients’ wrist rigidity as a hallmark for movement disorders. They found an inverse relationship between pulse width and voltage and reported that the minimum voltage value causing side effects increases as the pulse width decreases, thus concluding that DBS devices should be programmed with the shortest possible pulse duration. Moro and colleagues [34], instead, showed that the clinical benefits saturate above 3 V, while voltages above 3.6 V should be avoided because they result in an increased drain of the battery with no significant increment in the volume of neural elements excited. Finally, studies [35, 38] investigated the effects of the stimulation frequency on akinesia and rigidity in case of STN DBS. They reported that these symptoms reduce for frequencies above 50 Hz, the amount of symptom reduction increases almost linearly with the DBS frequency up to around 130 Hz, and the symptom reduction has a further small, nonlinear increase for frequencies from 130 Hz to 185 Hz.

The body of knowledge gained through these studies had a dual effect. On one side, it assisted with the formulation of the current protocols for DBS programming [10]. On the other, it contributed to formulate hypotheses about the therapeutic mechanisms of DBS [16, 39–41]. Specifically, since the largest clinical benefits were achieved with a combination of high frequency, short pulse width, and high voltage, it was hypothesized that the mechanisms of therapeutic DBS involve replacing the pathological rhythms of the basal ganglia output seen in PD with a tonic, high frequency (HF) firing. This increased activity

would prevent neurons from modulating the activity in their neighboring structures, thus creating an "*information lesion*" in the area [16, 39–41].

The scenario, though, has rapidly changed in the last few years. First, studies [26, 40, 42] have shown that non-Parkinsonian neural activity is irregular and low frequency. Second, pilot studies [43–45] have shown that carefully-designed non-regular, low-frequency stimulation patterns may have clinical merits comparable to those of high-frequency, regular DBS. Altogether, these studies suggest that (i) therapeutic mechanisms other than the information lesion are possible but need further investigation, and (ii) novel, low-power DBS solutions can be devised. These solutions could preserve the clinical benefits of current DBS therapies while addressing the major limitations of the current technology, e.g., the inefficient battery consumption, the need for lengthy manual programming, and the widespread influence on nearby cognitive loops with possible adverse side effects [46–51].

This invokes, however, for a deeper understanding of the dynamical interactions between nuclei in the cortico-basal ganglia-thalamo-cortical motor circuit (Fig. 2) in healthy and PD conditions, with and without DBS [9, 52]. It also invokes for the development of tools to optimize the stimulus waveforms and patterns, to use the battery power efficiently, and to robustly adapt the DBS input to the patient's neurological conditions.

4. CHALLENGES IN MODELING THE EFFECTS OF DBS

Neuronal networks in the brain communicate information about a subject's intent, internal state, and external environment through electrical activity. In PD, the lack of dopamine in the SNc is associated with pathological dynamics in the motor-related neuronal network spanning the cortico-basal ganglial-thalamo-cortical circuit (Fig. 2b), including pathological oscillations and synchronization [15]. Such dynamics are related to the manifestation of movement disorders including resting tremor, rigidity, and bradykinesia (slowness of movements) [27, 30].

DBS has been introduced to the clinical practice to interfere with pathological network dynamics and restore behavior [9]. From a systems perspective, DBS works as an exogenous localized control input into the network. It injects pulses of electrical current in well-defined anatomical sites (e.g., STN and GPi), but its effects spread throughout the entire network. Therapeutic DBS operates in open-loop and is typically high in power, which – although generally safe for the brain tissue [53] –leads to several problems: frequent surgical battery replacements, adverse side effects, and lack of adaptation of the stimulation to the patient's needs and symptoms' fluctuations [54, 55]. Moreover, high power stimulation does not restore network dynamics back to a healthy state, rather it appears to "block" certain regions (e.g., GPi) that are most pathological [41]. Since single neurons in the brain do not have sustained firing at high frequency (>100Hz) and high power signals in healthy conditions [26, 42], there is an important opportunity to restore network dynamics with low power DBS, thus minimizing adverse side effects and improving safety. Furthermore, since pathological signatures and severity may vary in different patients, there is a need for adapting the DBS input to the patient's own state, thus improving the potential therapeutic impact. To design adaptive low power signals, though, a predictive model of the affected neuronal networks

is required and a mathematically suitable framework for investigating innovative stimulation strategies must be formulated.

The research efforts reviewed in the next few sections pursued models that may generate activity in healthy and diseased conditions and may characterize the influence of DBS applied to specific target regions in the network. Some of these models also aimed to be amenable to analysis and simulation and were paired with control tools for designing computationally efficient DBS control strategies. The construction of models that satisfy all these features at the same time, though, remains an open-problem for several reasons:

- *System is distributed.* Networks involving brain structures are an interconnection of large groups of neuronal populations wherein information may be corrupted and communicated with delays.
- *Fundamental units in system are complex.* Single neurons are nonlinear multi-input single-output continuous-valued stochastic systems whose electrophysiological dynamics depend on the neuron type and location, the interconnections with other neurons, and, the signals provided by the extra- and intracellular environments.
- *System phenomena change nontrivially in the diseased state*. Pathological signatures such as synchronization and prominent oscillations typically arise in the diseased network and corrupt information transfer. These signatures may be localized in the network but have a global effect, which must be captured by the model.
- *DBS influences the system dynamics in a non-trivial way*. The underlying mechanisms of how DBS works and how it propagates through the network are not fully understood. DBS changes the extracellular environment in surrounding structures which in turn impacts the activity of each neuron, ultimately leading to a network effect. Different models have tried to capture these aspects with various degrees of success.
- *Supporting data is difficult to collect*. To construct a realistic model of the system, *in vivo* recordings from an entire neural circuit in healthy and diseased subjects, with and without DBS applied, must be obtained. These experiments are extremely difficult to perform and must be done with care on animals. Consequently, very few laboratories in the world have collected such data.

Current models of neurons and neuronal networks are predominantly biophysically-based and account for several factors that influence the electrophysiology of neurons, e.g., processing of synaptic input in the dendritic trees, ionic basis of electrical excitability, process of exogenous inputs such as the DBS signal [40, 56–60]. On the other hand, some models ignore subcellular neurophysiological data and biophysics, and represent the neuronal circuit as a network of phase oscillators to study phenomena such as synchronization [61–63]. These models do not account for biophysical factors such as short and long-term temporal dependencies that exist in spiking activity (e.g., refractoriness, bursting). However, they provide insight into network dynamics and may be more amenable for control design than biophysically-based models. Finally, several researchers have taken

a purely data-driven statistical modeling approach, where the key idea is to model only the timing between information-carrying events captured in neuronal network activity as opposed to modeling the biophysical mechanisms leading to spike generation. These critical events are sudden spikes in the neuronal transmembrane voltage, called "*action potentials*" [17, 64], which are modulated by both extrinsic factors (e.g., external stimuli, DBS signal) and intrinsic factors (e.g., neuron's own spiking history and that of neighboring neurons), and capture temporal dependencies observed in neuronal activity.

4.1. Biophysical Models

These models comprise single neuron elements which are variations of the Hodgkin-Huxley (HH) model [65]. The HH model is an equivalent electrical circuit (Fig. 3) of the membrane electrochemistry, which characterizes the membrane potential, V_m, of a neuron as a function of the trans-membrane ionic currents:

$$C_m \dot{V}_m + \sum_i g_i(V_m)(V_m - E_i) = I_e \quad (1)$$

The reversal potential for ion i, E_i, (also known as the Nernst potential) is the membrane potential at which there is no net flow of ions i from one side of the membrane to the other, and the conductances, the g_i's, depend nonlinearly on V_m and are determined experimentally. Typical expressions for sodium (Na) and potassium (K) conductances in the HH model are $g_{Na}(V_m) = g_{Na_{max}} m^3(V_m) h(V_m)$ and $g_K(V_m) = g_{k_{max}} n^4(V_m)$, respectively, where $\dot{s} = (s_\infty(V_m) - s)/\tau_s(V_m)$, $s = h, m, n$, and $s_\infty(V_m)$, $\tau_s(V_m)$ are monotonic functions for all s. With r types of ionic currents involved, the HH model for a single-compartmental neuron has at least $r + 1$ states. The DBS signal is typically modeled as an additive exogenous current, $I_e = I_{DBS}$, in equation (1) [40].

These models have been extremely useful for understanding the underlying mechanisms driving the cellular membrane voltage and have been used to introduce novel hypotheses about the mechanisms of therapeutic DBS. A model by Rubin and Terman [40] first introduced the notion of "*thalamic relay fidelity*" as a potential metric of success for DBS and provided a qualitative explanation of the therapeutic effects of high-frequency DBS by using bifurcation analysis. An expansion of the model introduced by Rubin and Terman was later used to disentangle the contributions of local cells in the subthalamo-pallidal sub-system (i.e., STN, GPe, and GPi) and fibers of passage to the modulation of thalamocortical neurons [59] while other models of the subthalamo-pallidal sub-system [56, 57, 60] highlighted the cellular mechanisms that may lead to a shift in rate and pattern of neurons in the basal ganglia under DBS. More recently, we developed a comprehensive network model of the interactions between the basal ganglia, the motor cortex, and the thalamus (Fig. 4), and we analyzed the effects of PD and DBS on the exchange between neurons across different structures [58]. Through numerical simulations, this model allowed to quantify the effects of DBS on multiple nested circuits as the frequency of stimulation increases. It demonstrated that high-frequency therapeutic DBS may evoke resonant effects over the cortico-basal ganglia-thalamo-cortical motor circuit. The model showed that the emergence of resonance depends on the frequency of DBS, modifies the global dynamics of the motor circuits,

and results in a general improvement of the metrics of functional neural activity (e.g., thalamic relay fidelity, power spectral content, etc.) that correlate with motor symptoms reduction, thus leading to the hypothesis that therapeutic DBS works by restoring the normal function and information processing capabilities of the motor circuit. Interestingly, this hypothesis overcomes the limitations of the information lesion theory [39–41], as it suggests that the therapeutic effects of HF DBS needs both the feedforward modulation of the pallido-thalamic pathway (which is accounted for by the information lesion theory) and the feedback modulation of the basal ganglia-cortico pathway to elicit resonance. Furthermore, it complements the information lesion theory as it shows that the high-frequency modulation of the pre-thalamic input restores the functional role of the thalamus in motor programming rather than leaving the thalamus in an inconsistent state. This is likely related to the nature of thalamocortical relay neurons, whose relay function depends on the temporal and spectral features of the presynaptic input [66]. It has been shown in [66], in fact, that different classes of presynaptic temporal patterns may result in similar relay performances and that both high-frequency oscillatory patterns (i.e., like those generated by GPi under high-frequency DBS) and irregular patterns (i.e., like those generated by GPi under healthy conditions) may result in similar relay fidelity values in thalamocortical relay neurons.

Interestingly, equation (1) captures the point-wise relationship between ionic current densities and membrane potential in a single point along the neuron's membrane [65, 67]. Models [40, 56–60] are denoted as "*single-compartment*" as they assume that a point-wise relationship like (1) is representative of the global behavior of an entire neuron or, at least, of its soma, thus neglecting the effects of the inhomogeneous distribution of ion channels, the gradient in membrane potential along the neuron's dendrites and axons, and the geometry of the DBS electrode.

Multi-compartment models [54, 68–70], instead, explicitly focus on the inhomogeneity of the neuron's membrane and surrounding medium. In these models, the point-wise equation (1) is used as a model-unit to be repeated as many times as the number of neuron's segments (a.k.a., "*compartments*") to be modeled, and the compartments are interconnected according to the neuron's own anatomy. Similarly, a finite-element description of the DBS electrode is paired with the neuron model and the anisotropy of the brain tissue is explicitly accounted for, thus resulting in a detailed three-dimensional representation of the interaction between the DBS-evoked electric field and the neuron. By encompassing a similar level of details, models have been used to investigate the local effects of DBS around the electrode and the complex electrochemical processes emerging at the interface between the DBS electrode and the nervous tissue as current is injected.

One caveat with the use of single- and multi-compartment biophysically-based models, though, is that they grow quickly in complexity as more neurons and segments are modeled, thus making analyses and the design of computationally efficient DBS control strategies intractable. Furthermore, parameters of these models are difficult to tune as they require intracellular measurements taken from single neurons *in vitro* via voltage, current or patch-clamp techniques [65, 67]. Therefore, several researchers have investigated other classes of models to describe and analyze the dynamics of neurons under PD conditions and DBS.

4.2. Mean-Field Models

Mean-field models have been explored as an alternative to biophysically-based neuron models to simulate and analyze the neural activity around the DBS lead. Defined in [71], these models tend to have a smaller number of state variables and equations than biophysically-based neuron models and capture the average electrophysiological activity of large, spatially-distributed ensembles of neurons, thus resulting amenable for both theoretical analysis and extensive simulations of large neural tissue layers.

The mean-field models proposed thus far to investigate the basal ganglia belong to the "neural mass" class (NM) [72], i.e., they primarily focus on the temporal dynamics of the basal ganglia and neglect spatial variability within each nucleus.

NM models have been extensively used to investigate the initiation of band-limited (e.g., beta-band) neural oscillations in the basal ganglia. Gillies and Willshaw [73, 74] proposed the following model template to describe the interaction between the average field potentials in the basal ganglia:

$$\tau_n \dot{x}_n = -x_n + \sum_j \alpha_{j \to n} \sigma_{j \to n}(x_j) + I_{e,n}(t) \tag{2}$$

where n is a generic nucleus in the basal ganglia (i.e., n = STN, GPe, etc.), x_n is the average field potential in the nucleus n, and $\sigma_{j \to n}(x_j)$ is a sigmoidal function that relates the average field potential x_j in the nucleus j to the average firing frequency of the neurons in the nucleus n. $I_{e,n}(t)$ provides a lump description of noise and external, non-specific inputs to the nucleus (e.g., input from secondary projections), and it can be expanded to include the DBS input. Finally, time constant τ_n and parameters $\alpha_{j \to n}$ must be estimated from data.

This model template was adopted in [74] to investigate the dynamics of the STN-GPe system and to show that oscillations consisting of bursts of high-frequency activity repeated at a low rate can be induced by increasing the inhibition of the GPe, which is typically observed in PD. Similarly, Modolo and colleagues [75] modified this model template to investigate the population effects of STN DBS and, through numerical simulations, they showed that low-frequency DBS (i.e., ≤ 20 Hz DBS) causes a phase-locking between the existing low-frequency pattern of the STN-GPe system and the DBS frequency, which determines an enhancement of the burstiness and synchrony across the STN. Vice versa, HF DBS gradually decreases the burstiness of the STN activity and promotes tonic oscillations, whose frequency saturates to 100 Hz.

Finally, Pavlides and colleagues [76] extended the modeling framework (2) to include the projections between the STN-GPe system, striatum, thalamus, and cortex. Through numerical simulations, they showed that pathologic, widespread beta-band oscillations can equally originate in the motor cortex or the STN-GPe system and then resonate throughout the basal ganglia. This modeling result is interesting because it suggests that the beta-band oscillations could be an emergent property of the entire motor circuit rather than a localized phenomenon. This would help to explain why the application of DBS in virtually any

structure along the motor circuit can eventually modulate the power of beta oscillations and deliver some amelioration of the symptoms of Parkinson's disease.

A different approach to NM modeling was taken instead in [77]. In this study, the stochastic-based dynamic causal modelling (DCM) framework [78] was used to investigate the spectral properties of large neural ensembles in the basal ganglia. Specifically, a DCM was fitted on measurements of auto- and cross-power spectra from the local field potentials of the STN, GPe, cortex, and striatum in a rodent model of PD. The model parameters were then analyzed to determine the effects of dopamine depletion on the connectivity between nuclei. Through this effort, authors demonstrated that chronic dopamine depletion reorganizes the motor circuit, i.e., it increases the effective connectivity between the cortex and the STN and decreases the connectivity from the STN to the GPe. Moreover, this study complements the results in [76] as it shows that, upon dopamine depletion, the effective connectivity along the indirect pathway may be relevant to the resonation of the beta-band oscillations.

Although amenable for computational and theoretical studies, these models often present limitations for control applications, as they typically focus on a single biomarker (e.g., beta-band oscillations) estimated under stationary conditions. However, recent experiments [31, 79] indicate that band-limited oscillations may equally emerge under healthy and PD conditions, are non-stationary, and may be modulated in frequency and pattern by the execution of movements. Overall, this suggests that multiple biomarkers should be simultaneously considered.

4.3. Oscillator Network Models

The dynamics of periodically spiking neurons has also been modeled with a network of phase oscillators, where each oscillator represents the phase of the membrane voltage, V, of a single neuron [61–63]. A population of N interacting phase oscillators subject to stimulation, S_j, and to random forces, F_j, obeys

$$\dot{\theta}_j = \omega - \frac{K}{N}\sum_{k=1}^{N} \sin(\theta_j - \theta_k) + \omega_j(t)S_j(\theta_j) + F_j(t) \quad (3)$$

where θ_j denotes the phase of the j-th phase oscillator. All oscillators have the same eigenfrequency ω and are globally coupled with strength $K > 0$. The impact of an electrical stimulus depends on the neuron's phase and is modeled by a 2π-periodic function such as $S_j(\theta_j) = I\cos(\theta_j)$ with intensity parameter I. $F_j(t)$ characterizes random forces modeled as Gaussian white noise [62, 63].

The study of large scale networks of oscillator models (3) has raised significant interest in the control theory and systems biology communities [80]. In PD, the emergence of pathological oscillations and synchronization in the 10–30Hz range in the STN, GPi, and cortex [24, 42] has inspired the use of oscillator networks to investigate the transition from a normal, desynchronized state to an abnormal, hyper-synchronous state. Perhaps more importantly, the theoretical framework provided by the oscillator model (3) has been highly amenable to design novel DBS patterns and closed-loop, adaptive DBS

paradigms. Early contributions by Tass and colleagues have suggested that DBS may be used to periodically reset the STN neurons and thus achieve a de-synchronized state [62, 63]. Furthermore, they suggested that local field potentials from the DBS electrode may be a proxy for the abnormal synchronization in the STN and that, by using the local field potentials as feedback variable in a closed-loop-controlled DBS configuration, it is possible to desynchronize the STN neurons through low-amplitude, non-pulsatile DBS currents [81, 82].

The idea of using DBS to reset a hyper-synchronized state has been further explored in recent years by introducing the notion of phase-response-curve (PRC). In a series of computational studies [83–85], Mohelis, Netoff, and colleagues have investigated metrics to characterize the level of synchronization in a large population of neurons and have proposed a closed-loop programming paradigm to maximally desynchronize the STN neuronal activity in PD patients. An example of the resultant model predictions is reported in Fig. 5.

One caveat with the model (3), though, is that precisely measuring the level of synchronization in a large population of neurons may be challenging with the currently implanted DBS electrodes, which may limit the practical application of the proposed methods [84]. Several studies have proposed local field potentials as a reliable proxy of the network activity [86, 87] but the variability of the field potential amplitude and frequency content across patients may hamper the translation of the proposed solutions.

4.4. Statistical Models

An alternative to the parametric models presented in the previous sections is provided by non-parametric, data-driven models estimated from spike trains recorded in PD patients during the DBS surgery or animal models of Parkinsonism. One of the most amenable mathematical formulations for spike trains is provided by point processes [88, 89]. Combined with generalized linear models and maximum likelihood estimation methods, point processes provide a modular modeling framework to capture higher order statistical properties of spike trains [90–92], quantify the effects of exogenous stimuli (e.g., sensorimotor feedback, DBS, etc.) on the spiking patterns of neurons [93], and reconstruct the functional connectivity between neurons in large networks [94].

A point process model (PPM) generalizes the rate of a Poisson process to one that is history dependent, and can characterize the relative contribution of intrinsic factors (e.g., spike history effects) and extrinsic factors (e.g., behavior, DBS, etc.) on the probability that a neuron will spike at any given time [89, 90]. Formally, a point process is a series of 0–1 random events that occur in continuous time. For a neural spike train, the 1s are individual spike times and the 0s are the times at which no spikes occur. To define a PPM of neural spiking activity, we consider an observation interval $(0, T]$ and let $\mathcal{N}(t)$ be the number of spikes counted in $(0, t]$ for $t \in (0, T]$. The PPM is then completely characterized by its conditional intensity function (CIF) λ_t defined as

$$\lambda_t(\mathcal{H}_t) = \lim_{\Delta \to 0} \frac{\mathcal{P}(\mathcal{N}(t+\Delta) - \mathcal{N}(t) = 1 \mid \mathcal{H}_t)}{\Delta} \quad (4)$$

where $\mathcal{H}_t$ denotes the history of spikes and any other variable that impacts spiking propensity up to time t (t is not included) and $\mathcal{P}$ is probability. It follows from (4) that the probability of a single spike in a small interval $(t, t+\Delta]$ is approximately $\mathcal{P}(\text{spike in } (t, t+\Delta] | \mathcal{H}_t \cong \lambda_t(\mathcal{H}_t)\Delta$.[89] For any realization of these processes, the sample path likelihood for the interval $(t_0, T]$,

$$\mathcal{L} = \exp\left(\int_{t_0}^{T} \log \lambda_u(\mathcal{H}_u)\, d\mathcal{N}(u) - \int_{t_0}^{T} \lambda_u(\mathcal{H}_u) du\right) \tag{5}$$

can be computed and used for static parameter estimation and model comparison[91]. Because the CIF completely characterizes a spike train, defining a model for the CIF defines a model for the spike train [88, 89].

In recent years, we proposed the use of point process models to characterize the response of neurons to DBS and account for certain features of neuronal firing like refractoriness, bursting and oscillations. In a series of seminal studies on the statistical properties of STN neurons from PD patients and primates, Sarma and colleagues [95–99] used point process models to discriminate healthy versus pathological discharge patterns, and quantify the effects of exogenous sensory stimuli on the subthalamic activity. A schematic of PPM for STN neurons under DBS is reported in Fig. 6. Filters $\mathcal{F}_1$ and $\mathcal{F}_2$ are linear and estimated from spike trains collected in PD patients or primates. Parameters in $\mathcal{F}_1$ and $\mathcal{F}_2$ are estimated by using the maximum likelihood method while the order and mathematical structure of the filters is chosen by maximizing the goodness-of-fit on the available data. Model parameters in $\mathcal{F}_1$ and $\mathcal{F}_2$ are then used to quantify the effects of exogenous sensory stimuli on the neuronal spiking pattern and to infer intrinsic neural dynamics like refractoriness, bursting, and rate oscillations.

A similar PPM-based approach was later applied to spike trains collected across the entire motor circuit (i.e., GPi, GPe, striatum, ventral and medial thalamus, motor, and sensory cortices) in non-human primates both before and after developing Parkinsonism, with and without STN DBS [100–105]. The analysis showed that, on average, neurons in different brain regions have similar responses to the DBS pulse, which may be a consequence of activating multiple neuronal circuits simultaneously, but the efficacy [106] of such response is generally low at non-therapeutic DBS frequencies. As the stimulation frequency increases, though, the efficacy significantly improves and reaches a peak value for DBS frequencies around 130Hz, which is a highly therapeutic frequency for non-human primates [107]. Furthermore, the analysis revealed that increments of the stimulation frequency are associated with increments in neural entrainment and complexity, i.e., ensembles of neurons under the same DBS input would spike in a more similar manner over time and the discharge patterns would be highly nonstationary. Overall, these results indicate that neurons across the entire cortico-basal ganglia-thalamo-cortical circuit may have an increased capability of transferring and processing information under DBS, which would compensate for the loss due to PD [108].

5. OPTIMIZING DBS THERAPY

All the modeling approaches presented thus far have contributed to investigate the cellular effects of electrical stimulation, to analyze the pathophysiology of PD, and to formulate novel hypotheses about the source of therapeutic merit for high-frequency regular DBS. These approaches have also resulted in numerical simulators of the cortico-basal ganglia-thalamo-cortical motor circuit with various degrees of complexity, resolution, and accuracy.

Simulators based on multi-compartment biophysically-based neuron models have been primarily used as computational testbeds to evaluate novel DBS pulse waveforms, electrode geometries, and stimulation modalities, e.g., current-versus voltage-controlled stimulation, unipolar-versus bipolar-stimulation, etc. [54, 109–113]. Perhaps more interestingly, these models have been used to optimize the DBS therapy at the level of individual patients by combining numerical simulations and medical imaging, Fig. 7. First, the detailed models of DBS electrode and neurons are used to carefully estimate the volume of neural tissue that is likely activated by a DBS pulse train. Then, the estimated volume is overlapped with reconstructed 3-D images of the patient's brain. Finally, the overlap between the estimated volume and the image-based reconstruction of the STN (for subthalamic DBS), GPi (for pallidal DBS), or ventrolateral thalamus (for thalamic DBS) is maximized. The maximization problem is solved by using convex optimization and machine-learning tools, and is formulated either at the time of DBS surgery [114, 115], i.e., when the trajectory of the electrode in the brain is planned and the final electrode position must be chosen, or at the time of DBS programming [116–121], i.e., when the electrode has been already implanted and the DBS pulse settings must be programmed.

Solutions [114–121] offer several advantages. First, they may assist clinicians during the DBS programming sessions and eventually reduce the duration of such sessions. Moreover, the proposed approaches can be advantageous as the number of contacts on a DBS electrode increases, thus enhancing the ability to customize the DBS-evoked electric field. Finally, the optimization process results in a patient-specific DBS program that can be applied in open-loop with no change to the current hardware, i.e., pulse generator and lead, Fig. 1. Possible limitations, instead, include the elevated computational cost of the optimization routines and multi-compartment model simulations, the cost for the integration of image processing and computational models, and the cost for gathering and harmonizing data from multiple sources at different stages of the DBS surgery, e.g., pre-surgery imaging, intraoperative recordings, etc.

Simulators based on single-compartment neuron models, instead, have been used in two distinct DBS design problems. One problem is the offline optimization of the DBS pattern, i.e., the goal is to design an optimal DBS pulse train that may be delivered in an open-loop configuration. Studies [44, 122] paired a model of the subthalamo-pallidal subsystem[40] with a genetic algorithm to optimize the DBS temporal pattern. In both studies, the goal of the optimization procedure was to maximize the relay reliability index [40], which measures the relay capability of the thalamocortical recipients of the subthalamo-pallidal subsystem. Results indicated that low-frequency, non-regular DBS patterns can (i) significantly improve the thalamic relay reliability over the baseline value under PD conditions and (ii) provide

results like therapeutic, high-frequency, regular DBS. Moreover, Brocker and colleagues [44] tested these optimized DBS patterns on both PD patients and rodent models of PD. Results showed that (1) the optimized DBS patterns were effective in the treatment of bradykinesia and tremor, i.e., two of the most impairing motor symptoms of PD, and (3) the average improvement in clinical ratings under DBS correlates well with the increments in relay reliability measured in the model under the same DBS input. Overall, these results suggest that non-periodic, low-frequency DBS patterns may be as effective as high-frequency, regular DBS but – to efficiently design such patterns – metrics must be introduced to quantify the effects of DBS on the dynamics of the cortico-basal ganglia-thalamo-cortical motor circuit.

The second problem involving single-compartment neuron models is the closed-loop regulation of DBS. Studies [123–129] have investigated potential feedback variables and model-based control strategies for DBS. A common trait of these studies is the focus on the pallido-thalamic interface, i.e., the synaptic currents from the GPi to thalamus are considered a proxy for the thalamic relay reliability and used as feedback variables. Different techniques have been proposed to design the controller (e.g., PID[124], model-predictive control [126], linear control [129], nonlinear control [128], etc.) and to estimate the synaptic input to thalamus by processing extracellular field potentials in the GPi. Despite the variety of control design techniques, though, all these studies aim to attenuate aberrant oscillations in the pallido-thalamic interaction, which has been suggested to deteriorate the thalamic relay reliability [66], and to restore a more normal activity across the cortico-basal ganglia-thalamo-cortical circuit. Furthermore, all the proposed solutions include a reference signal for the closed-loop scheme and design such signal off-line by simulating the single-compartment neuron models under non-PD conditions. Results from these studies consistently indicate that a non-pulsatile, non-periodic, low-amplitude DBS input can produce the same effects on the neural circuit as high-frequency DBS pulse trains while using a fraction of the energy required by the DBS pulse trains. Similar conclusions are derived in three studies [87, 129, 130] where the pulsatile nature of the DBS input is preserved, and the control strategy aims to adapt the amplitude and frequency of the DBS pulse train.

Overall, the main advantages of the proposed control solutions are (i) to impose a desired pattern to the neural activity while using a fraction of the power of current DBS programs and (ii) to adapt the stimulation to the actual state of the neurons in the cortico-basal ganglia-thalamo-cortical circuit. These results were later confirmed in PD patients [131, 132] and indicate that a closed-loop DBS therapy may be more energy-efficient and robust to motor fluctuations than open-loop DBS. Despite the success in early studies, though, model-based closed-loop DBS is still under investigation. The advantages in robustness, adaptivity, and energy-efficiency, in fact, are paired with the need for more sophisticate pulse generators, fast signal processing algorithms, and more computational power. Furthermore, the design of the reference signal is critical for the control performance and may cause unintended interference between the DBS input and neural dynamics that are completely unrelated to the PD condition [79].

6. CONCLUSIONS

Significant progress has been made in understanding and optimizing DBS in the last few years using systems approaches. Numerous models at different levels of detail and complexity have contributed to isolate potential factors to the therapeutic merit of high-frequency, regular DBS. Computational models have also fueled the investigation of novel, irregular and low-frequency DBS programs, thus leading to the important conclusion that the set of therapeutic DBS programs is overall larger than initially hypothesized. New tools and methods are therefore necessary to search this set and to systematically identify the most adequate DBS program for each patient. Furthermore, there is a growing interest in using these models to predict the therapeutic outcomes of novel electrode geometries. With the possibility of fabricating multipolar electrodes with a growing number of contacts, there is an opportunity to finely shape the electric field applied to the stimulation target and therefore models are required to carefully evaluate different contact configurations. Finally, the ability to model complex neuronal networks that span several brain nuclei offer a unique opportunity to evaluate novel stimulation targets, i.e., to simulate the effects of DBS on the neural circuits when the DBS electrode is placed in novel sites in the brain. These model-assisted therapies would help clinicians identify the most effective DBS location and program for each class of dominant motor symptoms and would lead to the development of quantitative criteria for planning the most adequate DBS surgery for each patient.

The proposed modeling frameworks have been often paired with model-based control techniques to design and evaluate closed-loop adaptive DBS strategies. The effort in designing control strategies for DBS has led in recent years to promising solutions that may help cope with the fluctuations of the PD conditions and neural variability. These solutions, though, still require further analysis to avoid unintended interactions with brain functions that are not affected by PD. Furthermore, the development of these solutions poses novel engineering challenges and design constraints on the stimulation devices, for which a thorough costs/benefits analysis is still required. Finally, these solutions are still in their early stages and need to translate from pre-clinical testing phases to clinical trials. This explains why the empirical evidence of the promised benefits is at the moment encouraging but still limited.

Acknowledgments

The authors would like to thank E. B. Montgomery Jr. and E. N. Eskandar for providing valuable data and discussions on the topic of DBS over the years. Work of authors in this field was supported by Burroughs Wellcome Fund CASI Award 1007274, NSF PECASE Award 1055560, and NIH Grant R01NS073118-02.

References

1. Miocinovic S, Somayajula S, Chitnis S, Vitek JL. History, applications, and mechanisms of deep brain stimulation. JAMA Neurol. 2013; 70: 163–71. [PubMed: 23407652]
2. Hickey P, Stacy M. Deep Brain Stimulation: A Paradigm Shifting Approach to Treat Parkinson's Disease. Front Neurosci. 2016; 10: 173. [PubMed: 27199637]
3. Holtzheimer PE, Kelley ME, Gross RE, Filkowski MM, Garlow SJ, Barrocas A, Wint D, Craighead MC, Kozarsky J, Chismar R, Moreines JL, Mewes K, Posse PR, Gutman DA, Mayberg HS. Subcallosal cingulate deep brain stimulation for treatment-resistant unipolar and bipolar depression. Arch Gen Psychiatry. 2012; 69: 150–8. [PubMed: 22213770]

4. Wu H, Van Dyck-Lippens PJ, Santegoeds R, van Kuyck K, Gabriels L, Lin G, Pan G, Li Y, Li D, Zhan S, Sun B, Nuttin B. Deep-brain stimulation for anorexia nervosa. World Neurosurg. 2013; 80: S29e1–10.
5. Ponce FA, Asaad WF, Foote KD, Anderson WS, Rees Cosgrove G, Baltuch GH, Beasley K, Reymers DE, Oh ES, Targum SD, Smith GS, Lyketsos CG, Lozano AM. for The ARG. Bilateral deep brain stimulation of the fornix for Alzheimer's disease: surgical safety in the ADvance trial. J Neurosurg. 2016; 125: 75–84. [PubMed: 26684775]
6. Fasano A, Appel-Cresswell S, Jog M, Zurowkski M, Duff-Canning S, Cohn M, Picillo M, Honey CR, Panisset M, Munhoz RP. Medical Management of Parkinson's Disease after Initiation of Deep Brain Stimulation. Can J Neurol Sci. 2016; 43: 626–34. [PubMed: 27670207]
7. Okun MS, Gallo BV, Mandybur G, Jagid J, Foote KD, Revilla FJ, Alterman R, Jankovic J, Simpson R, Junn F, Verhagen L, Arle JE, Ford B, Goodman RR, Stewart RM, Horn S, Baltuch GH, Kopell BH, Marshall F, Peichel D, Pahwa R, Lyons KE, Troster AI, Vitek JL, Tagliati M, Group SDS. Subthalamic deep brain stimulation with a constant-current device in Parkinson's disease: an open-label randomised controlled trial. Lancet Neurol. 2012; 11: 140–9. [PubMed: 22239915]
8. Rowland NC, Sammartino F, Lozano AM. Advances in surgery for movement disorders. Mov Disord. 2017; 32: 5–10. [PubMed: 27125681]
9. Benabid AL, Chabardes S, Mitrofanis J, Pollak P. Deep brain stimulation of the subthalamic nucleus for the treatment of Parkinson's disease. Lancet Neurol. 2009; 8: 67–81. [PubMed: 19081516]
10. Picillo M, Lozano AM, Kou N, Puppi Munhoz R, Fasano A. Programming Deep Brain Stimulation for Parkinson's Disease: The Toronto Western Hospital Algorithms. Brain Stimul. 2016; 9: 425–437. [PubMed: 26968806]
11. Goetz CG, Tilley BC, Shaftman SR, Stebbins GT, Fahn S, Martinez-Martin P, Poewe W, Sampaio C, Stern MB, Dodel R, Dubois B, Holloway R, Jankovic J, Kulisevsky J, Lang AE, Lees A, Leurgans S, LeWitt PA, Nyenhuis D, Olanow CW, Rascol O, Schrag A, Teresi JA, van Hilten JJ, LaPelle N. Movement Disorder Society URTF. Movement Disorder Society-sponsored revision of the Unified Parkinson's Disease Rating Scale (MDS-UPDRS): scale presentation and clinimetric testing results. Mov Disord. 2008; 23: 2129–70. [PubMed: 19025984]
12. Lowery, MM. Modeling Deep Brain Stimulation for Parkinson's Disease. In: Moustafa, AA, editor. Computational Models of Brain and Behavior. John Wiley & Sons, Ltd; 2017. 109–123.
13. Moro E, Lozano AM, Pollak P, Agid Y, Rehncrona S, Volkmann J, Kulisevsky J, Obeso JA, Albanese A, Hariz MI, Quinn NP, Speelman JD, Benabid AL, Fraix V, Mendes A, Welter ML, Houeto JL, Cornu P, Dormont D, Tornqvist AL, Ekberg R, Schnitzler A, Timmermann L, Wojtecki L, Gironell A, Rodriguez-Oroz MC, Guridi J, Bentivoglio AR, Contarino MF, Romito L, Scerrati M, Janssens M, Lang AE. Long-term results of a multicenter study on subthalamic and pallidal stimulation in Parkinson's disease. Mov Disord. 2010; 25: 578–86. [PubMed: 20213817]
14. DeLong MR, Wichmann T. Basal Ganglia Circuits as Targets for Neuromodulation in Parkinson Disease. JAMA Neurol. 2015; 72: 1354–60. [PubMed: 26409114]
15. Gale JT, Amirnovin R, Williams ZM, Flaherty AW, Eskandar EN. From symphony to cacophony: pathophysiology of the human basal ganglia in Parkinson disease. Neurosci Biobehav Rev. 2008; 32: 378–87. [PubMed: 17466375]
16. Montgomery EB Jr, Baker KB. Mechanisms of deep brain stimulation and future technical developments. Neurol Res. 2000; 22: 259–66. [PubMed: 10769818]
17. Kandel, E. Principles of Neural Science. 5. McGraw-Hill Education; 2013.
18. Haber SN, Calzavara R. The cortico-basal ganglia integrative network: the role of the thalamus. Brain Res Bull. 2009; 78: 69–74. [PubMed: 18950692]
19. Albin RL, Young AB, Penney JB. The functional anatomy of basal ganglia disorders. Trends Neurosci. 1989; 12: 366–75. [PubMed: 2479133]
20. Kreitzer AC. Physiology and pharmacology of striatal neurons. Annu Rev Neurosci. 2009; 32: 127–47. [PubMed: 19400717]
21. Wichmann T, Bergman H, DeLong MR. The primate subthalamic nucleus. III. Changes in motor behavior and neuronal activity in the internal pallidum induced by subthalamic inactivation in the MPTP model of parkinsonism. J Neurophysiol. 1994; 72: 521–30. [PubMed: 7983516]

22. Brown P, Oliviero A, Mazzone P, Insola A, Tonali P, Di Lazzaro V. Dopamine dependency of oscillations between subthalamic nucleus and pallidum in Parkinson's disease. J Neurosci. 2001; 21: 1033–8. [PubMed: 11157088]

23. Courtemanche R, Fujii N, Graybiel AM. Synchronous, focally modulated beta-band oscillations characterize local field potential activity in the striatum of awake behaving monkeys. J Neurosci. 2003; 23: 11741–52. [PubMed: 14684876]

24. Brown P. Abnormal oscillatory synchronisation in the motor system leads to impaired movement. Curr Opin Neurobiol. 2007; 17: 656–64. [PubMed: 18221864]

25. Gale, JT. PhD. 2004. Basis of periodic activities in the basal ganglia-thalamic-cortical system of the rhesus macaque. x, 202 leaves, bound

26. Gale JT, Shields DC, Jain FA, Amirnovin R, Eskandar EN. Subthalamic nucleus discharge patterns during movement in the normal monkey and Parkinsonian patient. Brain Res. 2009; 1260: 15–23. [PubMed: 19167367]

27. Kuhn AA, Tsui A, Aziz T, Ray N, Brucke C, Kupsch A, Schneider GH, Brown P. Pathological synchronisation in the subthalamic nucleus of patients with Parkinson's disease relates to both bradykinesia and rigidity. Exp Neurol. 2009; 215: 380–7. [PubMed: 19070616]

28. Levy R, Ashby P, Hutchison WD, Lang AE, Lozano AM, Dostrovsky JO. Dependence of subthalamic nucleus oscillations on movement and dopamine in Parkinson's disease. Brain. 2002; 125: 1196–209. [PubMed: 12023310]

29. Williams ZM, Neimat JS, Cosgrove GR, Eskandar EN. Timing and direction selectivity of subthalamic and pallidal neurons in patients with Parkinson disease. Exp Brain Res. 2005; 162: 407–16. [PubMed: 15635456]

30. Kuhn AA, Kupsch A, Schneider GH, Brown P. Reduction in subthalamic 8–35 Hz oscillatory activity correlates with clinical improvement in Parkinson's disease. Eur J Neurosci. 2006; 23: 1956–60. [PubMed: 16623853]

31. Tinkhauser G, Pogosyan A, Little S, Beudel M, Herz DM, Tan H, Brown P. The modulatory effect of adaptive deep brain stimulation on beta bursts in Parkinson's disease. Brain. 2017; 140: 1053–1067. [PubMed: 28334851]

32. Pessiglione M, Guehl D, Rolland AS, Francois C, Hirsch EC, Feger J, Tremblay L. Thalamic neuronal activity in dopamine-depleted primates: evidence for a loss of functional segregation within basal ganglia circuits. J Neurosci. 2005; 25: 1523–31. [PubMed: 15703406]

33. Schneider JS, Rothblat DS. Alterations in intralaminar and motor thalamic physiology following nigrostriatal dopamine depletion. Brain Res. 1996; 742: 25–33. [PubMed: 9117401]

34. Moro E, Esselink RJ, Xie J, Hommel M, Benabid AL, Pollak P. The impact on Parkinson's disease of electrical parameter settings in STN stimulation. Neurology. 2002; 59: 706–13. [PubMed: 12221161]

35. Volkmann J, Herzog J, Kopper F, Deuschl G. Introduction to the programming of deep brain stimulators. Mov Disord. 2002; 17 (Suppl 3) S181–7. [PubMed: 11948775]

36. Rizzone M, Lanotte M, Bergamasco B, Tavella A, Torre E, Faccani G, Melcarne A, Lopiano L. Deep brain stimulation of the subthalamic nucleus in Parkinson's disease: effects of variation in stimulation parameters. J Neurol Neurosurg Psychiatry. 2001; 71: 215–9. [PubMed: 11459896]

37. Deep-Brain Stimulation for Parkinson's Disease Study G. Obeso JA, Olanow CW, Rodriguez-Oroz MC, Krack P, Kumar R, Lang AE. Deep-brain stimulation of the subthalamic nucleus or the pars interna of the globus pallidus in Parkinson's disease. N Engl J Med. 2001; 345: 956–63. [PubMed: 11575287]

38. Limousin P, Pollak P, Benazzouz A, Hoffmann D, Le Bas JF, Broussolle E, Perret JE, Benabid AL. Effect of parkinsonian signs and symptoms of bilateral subthalamic nucleus stimulation. Lancet. 1995; 345: 91–5. [PubMed: 7815888]

39. Dorval AD, Russo GS, Hashimoto T, Xu W, Grill WM, Vitek JL. Deep brain stimulation reduces neuronal entropy in the MPTP-primate model of Parkinson's disease. J Neurophysiol. 2008; 100: 2807–18. [PubMed: 18784271]

40. Rubin JE, Terman D. High frequency stimulation of the subthalamic nucleus eliminates pathological thalamic rhythmicity in a computational model. J Comput Neurosci. 2004; 16: 211–35. [PubMed: 15114047]

41. Grill WM, Snyder AN, Miocinovic S. Deep brain stimulation creates an informational lesion of the stimulated nucleus. Neuroreport. 2004; 15: 1137–40. [PubMed: 15129161]
42. Raz A, Vaadia E, Bergman H. Firing patterns and correlations of spontaneous discharge of pallidal neurons in the normal and the tremulous 1-methyl-4-phenyl-1,2,3,6-tetrahydropyridine vervet model of parkinsonism. J Neurosci. 2000; 20: 8559–71. [PubMed: 11069964]
43. Brocker DT, Swan BD, Turner DA, Gross RE, Tatter SB, Koop MM, Bronte-Stewart H, Grill WM. Improved efficacy of temporally non-regular deep brain stimulation in Parkinson's disease. Exp Neurol. 2013; 239: 60–7. [PubMed: 23022917]
44. Brocker DT, Swan BD, So RQ, Turner DA, Gross RE, Grill WM. Optimized temporal pattern of brain stimulation designed by computational evolution. Sci Transl Med. 2017. 9.
45. Akbar U, Raike RS, Hack N, Hess CW, Skinner J, Martinez-Ramirez D, DeJesus S, Okun MS. Randomized, Blinded Pilot Testing of Nonconventional Stimulation Patterns and Shapes in Parkinson's Disease and Essential Tremor: Evidence for Further Evaluating Narrow and Biphasic Pulses. Neuromodulation. 2016; 19: 343–56. [PubMed: 27000764]
46. Wojtecki L, Timmermann L, Jorgens S, Sudmeyer M, Maarouf M, Treuer H, Gross J, Lehrke R, Koulousakis A, Voges J, Sturm V, Schnitzler A. Frequency-dependent reciprocal modulation of verbal fluency and motor functions in subthalamic deep brain stimulation. Arch Neurol. 2006; 63: 1273–6. [PubMed: 16966504]
47. De Gaspari D, Siri C, Di Gioia M, Antonini A, Isella V, Pizzolato A, Landi A, Vergani F, Gaini SM, Appollonio IM, Pezzoli G. Clinical correlates and cognitive underpinnings of verbal fluency impairment after chronic subthalamic stimulation in Parkinson's disease. Parkinsonism Relat Disord. 2006; 12: 289–95. [PubMed: 16554183]
48. Le Jeune F, Peron J, Grandjean D, Drapier S, Haegelen C, Garin E, Millet B, Verin M. Subthalamic nucleus stimulation affects limbic and associative circuits: a PET study. Eur J Nucl Med Mol Imaging. 2010; 37: 1512–20. [PubMed: 20349231]
49. Selzler K, Burack M, Bender R, Mapstone M. Neurophysiological correlates of motor and working memory performance following subthalamic nucleus stimulation. J Cogn Neurosci. 2013; 25: 37–48. [PubMed: 23198889]
50. Temel Y, Blokland A, Ackermans L, Boon P, van Kranen-Mastenbroek VH, Beuls EA, Spincemaille GH, Visser-Vandewalle V. Differential effects of subthalamic nucleus stimulation in advanced Parkinson disease on reaction time performance. Exp Brain Res. 2006; 169: 389–99. [PubMed: 16273395]
51. Munhoz RP, Picillo M, Fox SH, Bruno V, Panisset M, Honey CR, Fasano A. Eligibility Criteria for Deep Brain Stimulation in Parkinson's Disease, Tremor, and Dystonia. Can J Neurol Sci. 2016; 43: 462–71. [PubMed: 27139127]
52. Perlmutter JS, Mink JW. Deep brain stimulation. Annu Rev Neurosci. 2006; 29: 229–57. [PubMed: 16776585]
53. Moss J, Ryder T, Aziz TZ, Graeber MB, Bain PG. Electron microscopy of tissue adherent to explanted electrodes in dystonia and Parkinson's disease. Brain. 2004; 127: 2755–63. [PubMed: 15329356]
54. Butson CR, McIntyre CC. Current steering to control the volume of tissue activated during deep brain stimulation. Brain Stimul. 2008; 1: 7–15. [PubMed: 19142235]
55. Wei XF, Grill WM. Impedance characteristics of deep brain stimulation electrodes in vitro and in vivo. J Neural Eng. 2009; 6: 046008. [PubMed: 19587394]
56. Santaniello, S; Fiengo, G; Glielmo, L; Grill, WM. Basal Ganglia Modeling in Healthy and Parkinson's Disease State. II. Network-based Multi-Units Simulation. 2007 American Control Conference; 2007; 4095–4100.
57. Santaniello, S; Fiengo, G; Glielmo, L; Grill, WM. Basal Ganglia Modeling in Healthy and Parkinson's Disease State. I. Isolated Neurons Activity. 2007 American Control Conference; 2007; 4089–4094.
58. Santaniello S, McCarthy MM, Montgomery EB Jr, Gale JT, Kopell N, Sarma SV. Therapeutic mechanisms of high-frequency stimulation in Parkinson's disease and neural restoration via loop-based reinforcement. Proc Natl Acad Sci U S A. 2015; 112: E586–95. [PubMed: 25624501]

59. So RQ, Kent AR, Grill WM. Relative contributions of local cell and passing fiber activation and silencing to changes in thalamic fidelity during deep brain stimulation and lesioning: a computational modeling study. J Comput Neurosci. 2012; 32: 499–519. [PubMed: 21984318]
60. Hahn PJ, McIntyre CC. Modeling shifts in the rate and pattern of subthalamopallidal network activity during deep brain stimulation. J Comput Neurosci. 2010; 28: 425–41. [PubMed: 20309620]
61. Ermentrout GB, Kopell N. Multiple pulse interactions and averaging in systems of coupled neural oscillators. Journal of Mathematical Biology. 1991; 29: 195–217.
62. Tass PA. A model of desynchronizing deep brain stimulation with a demand-controlled coordinated reset of neural subpopulations. Biol Cybern. 2003; 89: 81–8. [PubMed: 12905037]
63. Tass PA, Hauptmann C. Therapeutic modulation of synaptic connectivity with desynchronizing brain stimulation. Int J Psychophysiol. 2007; 64: 53–61. [PubMed: 16997408]
64. Brodal, P. The central nervous system. 5. New York, NY, United States of America: Oxford University Press; 2016.
65. Hodgkin AL, Huxley AF. A quantitative description of membrane current and its application to conduction and excitation in nerve. J Physiol. 1952; 117: 500–44. [PubMed: 12991237]
66. Agarwal R, Sarma SV. Performance limitations of relay neurons. PLoS Comput Biol. 2012; 8: e1002626. [PubMed: 22973184]
67. Neher E, Sakmann B. The patch clamp technique. Sci Am. 1992; 266: 44–51. [PubMed: 1374932]
68. McIntyre CC, Grill WM, Sherman DL, Thakor NV. Cellular effects of deep brain stimulation: model-based analysis of activation and inhibition. J Neurophysiol. 2004; 91: 1457–69. [PubMed: 14668299]
69. Miocinovic S, Parent M, Butson CR, Hahn PJ, Russo GS, Vitek JL, McIntyre CC. Computational analysis of subthalamic nucleus and lenticular fasciculus activation during therapeutic deep brain stimulation. J Neurophysiol. 2006; 96: 1569–80. [PubMed: 16738214]
70. Kent AR, Grill WM. Neural origin of evoked potentials during thalamic deep brain stimulation. J Neurophysiol. 2013; 110: 826–43. [PubMed: 23719207]
71. Ermentrout GB. Neural networks as spatio-temporal pattern-forming systems. Rep Prog Phys. 1998; 61: 353.
72. Pinotsis D, Robinson P, Beim Graben P, Friston K. Neural masses and fields: modeling the dynamics of brain activity. Front Comput Neurosci. 2014; 8: 149. [PubMed: 25477813]
73. Gillies AJ, Willshaw DJ. A massively connected subthalamic nucleus leads to the generation of widespread pulses. Proc Biol Sci. 1998; 265: 2101–9. [PubMed: 9842737]
74. Gillies A, Willshaw D, Li Z. Subthalamic-pallidal interactions are critical in determining normal and abnormal functioning of the basal ganglia. Proc Biol Sci. 2002; 269: 545–51. [PubMed: 11916469]
75. Modolo J, Henry J, Beuter A. Dynamics of the subthalamo-pallidal complex in Parkinson's disease during deep brain stimulation. J Biol Phys. 2008; 34: 251–66. [PubMed: 19669474]
76. Pavlides A, Hogan SJ, Bogacz R. Computational Models Describing Possible Mechanisms for Generation of Excessive Beta Oscillations in Parkinson's Disease. PLoS Comput Biol. 2015; 11: e1004609. [PubMed: 26683341]
77. Moran RJ, Mallet N, Litvak V, Dolan RJ, Magill PJ, Friston KJ, Brown P. Alterations in brain connectivity underlying beta oscillations in Parkinsonism. PLoS Comput Biol. 2011; 7: e1002124. [PubMed: 21852943]
78. Moran RJ, Kiebel SJ, Stephan KE, Reilly RB, Daunizeau J, Friston KJ. A neural mass model of spectral responses in electrophysiology. Neuroimage. 2007; 37: 706–20. [PubMed: 17632015]
79. Johnson LA, Nebeck SD, Muralidharan A, Johnson MD, Baker KB, Vitek JL. Closed-Loop Deep Brain Stimulation Effects on Parkinsonian Motor Symptoms in a Non-Human Primate - Is Beta Enough? Brain Stimul. 2016; 9: 892–896. [PubMed: 27401045]
80. Stiefel KM, Ermentrout GB. Neurons as oscillators. J Neurophysiol. 2016; 116: 2950–2960. [PubMed: 27683887]
81. Popovych OV, Hauptmann C, Tass PA. Control of neuronal synchrony by nonlinear delayed feedback. Biol Cybern. 2006; 95: 69–85. [PubMed: 16614837]

82. Popovych OV, Tass PA. Synchronization control of interacting oscillatory ensembles by mixed nonlinear delayed feedback. Phys Rev E Stat Nonlin Soft Matter Phys. 2010; 82: 026204. [PubMed: 20866890]
83. Holt AB, Netoff TI. Origins and suppression of oscillations in a computational model of Parkinson's disease. J Comput Neurosci. 2014; 37: 505–21. [PubMed: 25099916]
84. Holt AB, Wilson D, Shinn M, Moehlis J, Netoff TI. Phasic Burst Stimulation: A Closed-Loop Approach to Tuning Deep Brain Stimulation Parameters for Parkinson's Disease. PLoS Comput Biol. 2016; 12: e1005011. [PubMed: 27415832]
85. Snari R, Tinsley MR, Wilson D, Faramarzi S, Netoff TI, Moehlis J, Showalter K. Desynchronization of stochastically synchronized chemical oscillators. Chaos. 2015; 25: 123116. [PubMed: 26723155]
86. Kent AR, Swan BD, Brocker DT, Turner DA, Gross RE, Grill WM. Measurement of evoked potentials during thalamic deep brain stimulation. Brain Stimul. 2015; 8: 42–56. [PubMed: 25457213]
87. Santaniello S, Fiengo G, Glielmo L, Grill WM. Closed-loop control of deep brain stimulation: a simulation study. IEEE Trans Neural Syst Rehabil Eng. 2011; 19: 15–24. [PubMed: 20889437]
88. Snyder, DL, Miller, MI, Snyder, DL. Random point processes in time and space. 2. New York: Springer-Verlag; 1991.
89. Kass, RE, Eden, UT, Brown, EN. Analysis of neural data. New York, NY ; Heidelberg ; Dordrecht ; London: Springer; 2014.
90. Barbieri R, Quirk MC, Frank LM, Wilson MA, Brown EN. Construction and analysis of non-Poisson stimulus-response models of neural spiking activity. J Neurosci Methods. 2001; 105: 25–37. [PubMed: 11166363]
91. Brown, EN, Barbieri, R, Eden, UT, Frank, LM. Likelihood methods for neural spike train data analysis. In: Feng, J, editor. Computational Neuroscience: A Comprehensive Approach. 1. London, UK: Chapman and Hall/CRC; 2003. 253–89.
92. Coleman TP, Sarma SS. A computationally efficient method for nonparametric modeling of neural spiking activity with point processes. Neural Comput. 2010; 22: 2002–30. [PubMed: 20438334]
93. Truccolo W, Eden UT, Fellows MR, Donoghue JP, Brown EN. A point process framework for relating neural spiking activity to spiking history, neural ensemble, and extrinsic covariate effects. J Neurophysiol. 2005; 93: 1074–89. [PubMed: 15356183]
94. Chen Z, Putrino DF, Ghosh S, Barbieri R, Brown EN. Statistical inference for assessing functional connectivity of neuronal ensembles with sparse spiking data. IEEE Trans Neural Syst Rehabil Eng. 2011; 19: 121–35. [PubMed: 20937583]
95. Pedoto G, Santaniello S, Fiengo G, Glielmo L, Hallett M, Zhuang P, Sarma SV. Point process modeling reveals anatomical non-uniform distribution across the subthalamic nucleus in Parkinson's disease. Conf Proc IEEE Eng Med Biol Soc. 2012; 2012: 2539–42.
96. Sarma SV, Cheng ML, Eden U, Williams Z, Brown EN, Eskandar E. The effects of cues on neurons in the basal ganglia in Parkinson's disease. Front Integr Neurosci. 2012; 6: 40. [PubMed: 22855673]
97. Sarma, SV; Eden, UT; Cheng, ML; Williams, Z; Eskandar, EN; Brown, EN. Using point process models to determine the impact of visual cues on basal ganglia activity and behavior of Parkinson's patients. Proceedings of the 48h IEEE Conference on Decision and Control (CDC) held jointly with 2009 28th Chinese Control Conference; 2009; 7716–7722.
98. Sarma SV, Eden UT, Cheng ML, Williams ZM, Hu R, Eskandar E, Brown EN. Using point process models to compare neural spiking activity in the subthalamic nucleus of Parkinson's patients and a healthy primate. IEEE Trans Biomed Eng. 2010; 57: 1297–305. [PubMed: 20172804]
99. Sarma, SV; Cheng, M; Eden, U; Hu, R; Williams, Z; Brown, EN; Eskandar, E. Modeling neural spiking activity in the sub-thalamic nucleus of Parkinson's patients and a healthy primate. 2008 47th IEEE Conference on Decision and Control; 2008; 2012–2017.
100. Santaniello S, Gale JT, Montgomery EB Jr, Sarma SV. Reinforcement mechanisms in putamen during high frequency STN DBS: A point process study. Conf Proc IEEE Eng Med Biol Soc. 2012; 2012: 1214–7.

101. Santaniello S, Gale JT, Montgomery EB, Sarma SV. Modeling the motor striatum under Deep Brain Stimulation in normal and MPTP conditions. Conf Proc IEEE Eng Med Biol Soc. 2010; 2010: 2065–8.
102. Santaniello S, Gale JT, Montgomery EB, Sarma SV. Modeling the effects of Deep Brain Stimulation on sensorimotor cortex in normal and MPTP conditions. Conf Proc IEEE Eng Med Biol Soc. 2010; 2010: 2081–4.
103. Santaniello S, Montgomery EB Jr, Gale JT, Sarma SV. Non-stationary discharge patterns in motor cortex under subthalamic nucleus deep brain stimulation. Front Integr Neurosci. 2012; 6: 35. [PubMed: 22754509]
104. Saxena S, Santaniello S, Montgomery EB, Gale JT, Sarma SV. Point process models show temporal dependencies of basal ganglia nuclei under deep brain stimulation. Conf Proc IEEE Eng Med Biol Soc. 2010; 2010: 4152–5.
105. Deng C, Sun T, Manning Z, Gale JT, Montgomery EB, Santaniello S. Effects of the temporal pattern of subthalamic deep brain stimulation on the neuronal complexity in the globus pallidus. Conf Proc IEEE Eng Med Biol Soc. 2017; 2017: 3352–3355.
106. Montgomery EB Jr. Effects of GPi stimulation on human thalamic neuronal activity. Clin Neurophysiol. 2006; 117: 2691–702. [PubMed: 17029953]
107. Hashimoto T, Elder CM, Okun MS, Patrick SK, Vitek JL. Stimulation of the subthalamic nucleus changes the firing pattern of pallidal neurons. J Neurosci. 2003; 23: 1916–23. [PubMed: 12629196]
108. Vyas S, Huang H, Gale JT, Sarma SV, Montgomery EB. Neuronal Complexity in Subthalamic Nucleus is Reduced in Parkinson's Disease. IEEE Trans Neural Syst Rehabil Eng. 2016; 24: 36–45. [PubMed: 26168436]
109. Wei XF, Grill WM. Current density distributions, field distributions and impedance analysis of segmented deep brain stimulation electrodes. J Neural Eng. 2005; 2: 139–47. [PubMed: 16317238]
110. Lai HY, Liao LD, Lin CT, Hsu JH, He X, Chen YY, Chang JY, Chen HF, Tsang S, Shih YY. Design, simulation and experimental validation of a novel flexible neural probe for deep brain stimulation and multichannel recording. J Neural Eng. 2012; 9: 036001. [PubMed: 22488106]
111. Howell B, Grill WM. Evaluation of high-perimeter electrode designs for deep brain stimulation. J Neural Eng. 2014; 11: 046026. [PubMed: 25029124]
112. Howell B, Huynh B, Grill WM. Design and in vivo evaluation of more efficient and selective deep brain stimulation electrodes. J Neural Eng. 2015; 12: 046030. [PubMed: 26170244]
113. Willsie AC, Dorval AD. Computational Field Shaping for Deep Brain Stimulation With Thousands of Contacts in a Novel Electrode Geometry. Neuromodulation. 2015; 18: 542–50. [PubMed: 26245306]
114. Butson CR, Cooper SE, Henderson JM, McIntyre CC. Patient-specific analysis of the volume of tissue activated during deep brain stimulation. Neuroimage. 2007; 34: 661–70. [PubMed: 17113789]
115. Butson CR, Cooper SE, Henderson JM, Wolgamuth B, McIntyre CC. Probabilistic analysis of activation volumes generated during deep brain stimulation. Neuroimage. 2011; 54: 2096–104. [PubMed: 20974269]
116. Frankemolle AM, Wu J, Noecker AM, Voelcker-Rehage C, Ho JC, Vitek JL, McIntyre CC, Alberts JL. Reversing cognitive-motor impairments in Parkinson's disease patients using a computational modelling approach to deep brain stimulation programming. Brain. 2010; 133: 746–61. [PubMed: 20061324]
117. Lehto LJ, Slopsema JP, Johnson MD, Shatillo A, Teplitzky BA, Utecht L, Adriany G, Mangia S, Sierra A, Low WC, Grohn O, Michaeli S. Orientation selective deep brain stimulation. J Neural Eng. 2017; 14: 016016. [PubMed: 28068296]
118. Pena E, Zhang S, Deyo S, Xiao Y, Johnson MD. Particle swarm optimization for programming deep brain stimulation arrays. J Neural Eng. 2017; 14: 016014. [PubMed: 28068291]
119. Shamir RR, Dolber T, Noecker AM, Walter BL, McIntyre CC. Machine Learning Approach to Optimizing Combined Stimulation and Medication Therapies for Parkinson's Disease. Brain Stimul. 2015; 8: 1025–32. [PubMed: 26140956]

120. Shamir RR, Dolbert T, Noecker AM, Frankemolle AM, Walter BL, McIntyre CC. A method for predicting the outcomes of combined pharmacologic and deep brain stimulation therapy for Parkinson's disease. Med Image Comput Comput Assist Interv. 2014; 17: 188–95. [PubMed: 25485378]

121. Xiao Y, Pena E, Johnson MD. Theoretical Optimization of Stimulation Strategies for a Directionally Segmented Deep Brain Stimulation Electrode Array. IEEE Trans Biomed Eng. 2016; 63: 359–71. [PubMed: 26208259]

122. Feng XJ, Shea-Brown E, Greenwald B, Kosut R, Rabitz H. Optimal deep brain stimulation of the subthalamic nucleus--a computational study. J Comput Neurosci. 2007; 23: 265–82. [PubMed: 17484043]

123. Agarwal R, Sarma SV. Restoring the basal ganglia in Parkinson's disease to normal via multi-input phase-shifted deep brain stimulation. Conf Proc IEEE Eng Med Biol Soc. 2010; 2010: 1539–42.

124. Gorzelic P, Schiff SJ, Sinha A. Model-based rational feedback controller design for closed-loop deep brain stimulation of Parkinson's disease. J Neural Eng. 2013; 10: 026016. [PubMed: 23449002]

125. Grant PF, Lowery MM. Simulation of cortico-basal ganglia oscillations and their suppression by closed loop deep brain stimulation. IEEE Trans Neural Syst Rehabil Eng. 2013; 21: 584–94. [PubMed: 22695362]

126. Liu C, Wang J, Deng B, Wei X, Yu H, Li H, Fietkiewicz C, Loparo KA. Closed-Loop Control of Tremor-Predominant Parkinsonian State Based on Parameter Estimation. IEEE Trans Neural Syst Rehabil Eng. 2016; 24: 1109–1121. [PubMed: 26955042]

127. Liu C, Wang J, Li H, Lu M, Deng B, Yu H, Wei X, Fietkiewicz C, Loparo KA. Closed-Loop Modulation of the Pathological Disorders of the Basal Ganglia Network. IEEE Trans Neural Netw Learn Syst. 2017; 28: 371–382. [PubMed: 26766381]

128. Liu J, Khalil HK, Oweiss KG. Model-based analysis and control of a network of basal ganglia spiking neurons in the normal and parkinsonian states. J Neural Eng. 2011; 8: 045002. [PubMed: 21775788]

129. Huang HD, Santaniello S. Closed-loop low-frequency DBS restores thalamocortical relay fidelity in a computational model of the motor loop. Conf Proc IEEE Eng Med Biol Soc. 2017; 2017: 1954–1957.

130. Popovych OV, Lysyansky B, Tass PA. Closed-loop deep brain stimulation by pulsatile delayed feedback with increased gap between pulse phases. Sci Rep. 2017; 7: 1033. [PubMed: 28432303]

131. Little S, Pogosyan A, Neal S, Zavala B, Zrinzo L, Hariz M, Foltynie T, Limousin P, Ashkan K, FitzGerald J, Green AL, Aziz TZ, Brown P. Adaptive deep brain stimulation in advanced Parkinson disease. Ann Neurol. 2013; 74: 449–57. [PubMed: 23852650]

132. Arlotti M, Rossi L, Rosa M, Marceglia S, Priori A. An external portable device for adaptive deep brain stimulation (aDBS) clinical research in advanced Parkinson's Disease. Med Eng Phys. 2016; 38: 498–505. [PubMed: 27029510]

133. McIntyre CC, Chaturvedi A, Shamir RR, Lempka SF. Engineering the next generation of clinical deep brain stimulation technology. Brain Stimul. 2015; 8: 21–6. [PubMed: 25161150]

SIDEBAR

Parkinson's disease (PD) is the second-most common neurodegenerative disorder in the United States after Alzheimer's disease. Prevalence of PD is estimated around 0.3% of the general population, with rates increasing to 1–2% and 4–5% for individuals over age 65 and 85, respectively. Major motor symptoms of PD include bradykinesia (i.e., slowness of voluntary movements), rigidity, tremor, and postural instability. The severity of these symptoms increases as the disease progresses. Current treatments help alleviate symptomatic effects, but no available treatments have been proven to cure or slow disease progression. DBS is typically recommended to PD patients who are still responsive to anti-PD medications but have developed medication-induced dyskinesia. On average, patients undergoing the DBS surgery are at relatively advanced stages of the disease, with severe motor complications and a mean disease duration of 12 to 15 years. By adding DBS therapy, these late-stage PD patients may better manage the dyskinesia and other motor complications, reduce their dosages of anti-PD medications by 30–50% on average, and overall prolong the management of PD symptoms.

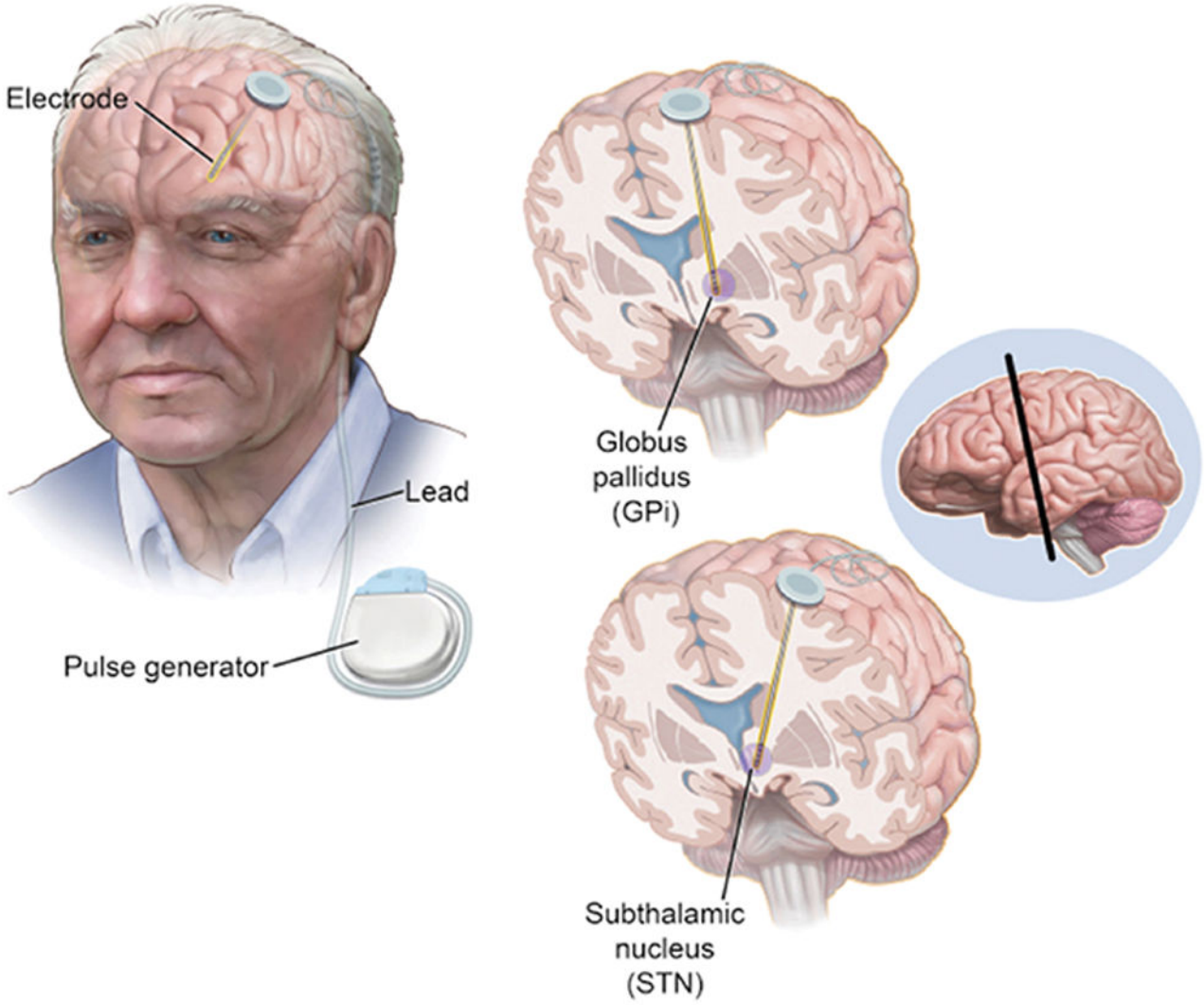

Figure 1.

Schematic of the chronic deep brain stimulation implant and devices for the treatment of Parkinson's disease. An electrode is surgically implanted either in the subthalamic nucleus (STN) or the internal globus pallidus (GPi) and connected to an implanted pulse generator through subcutaneous wires. The pulse generator is programmed to deliver charge-balanced, voltage-controlled electric pulses. Typical duration of the anodic part of each pulse is 60–90 μs and pulse amplitude is 2–3V. Image reproduced from (Hickey & Stacy, 2016) [2] under the Creative Commons Attribution License (CC BY).

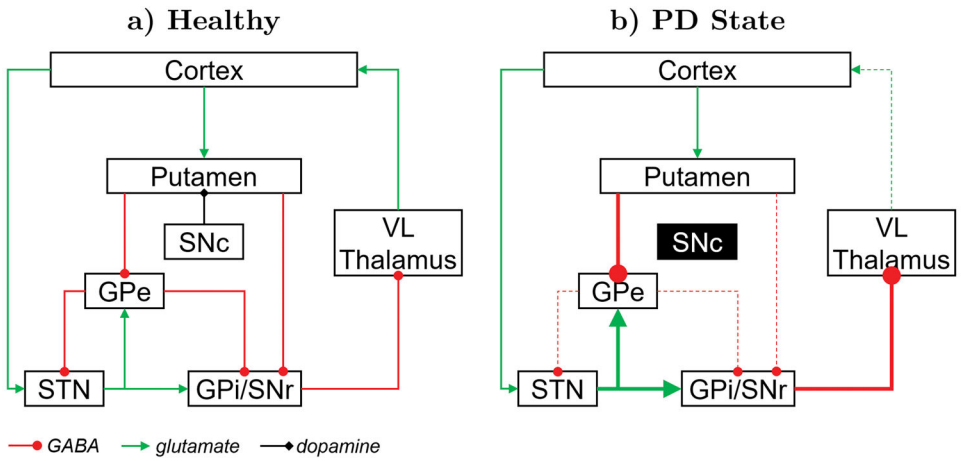

Figure 2.

A–B) Classic model of the basal ganglia in healthy (A) and parkinsonian (B) conditions. Cortex provides excitatory glutamatergic projections to the putamen (a part of striatum), which sends GABAergic inhibitory projections to the GPi and the SNr by two pathways: the “direct circuit” (putamen-GPi) and the “indirect circuit” (putamen-GPe-STN-GPi/SNr). Dopamine from the SNc facilitates striatal neurons in the direct pathway and inhibits those in the indirect pathway. In Parkinson’s disease (B), dopamine depletion causes hyper-activity along the indirect circuit and hypo-activity along the direct circuit. Green, red, and black arrows denote excitatory (i.e., glutamatergic), inhibitory (i.e., GABAergic), and dopaminergic projections, respectively. Thick and thin-dashed arrows indicate hyper- and hypo-activity, respectively. Legend: VL = ventrolateral; GPe (GPi) = external (internal) globus pallidus; STN = subthalamic nucleus; SNr (SNc) = substantial nigra pars reticulata (pars compacta).

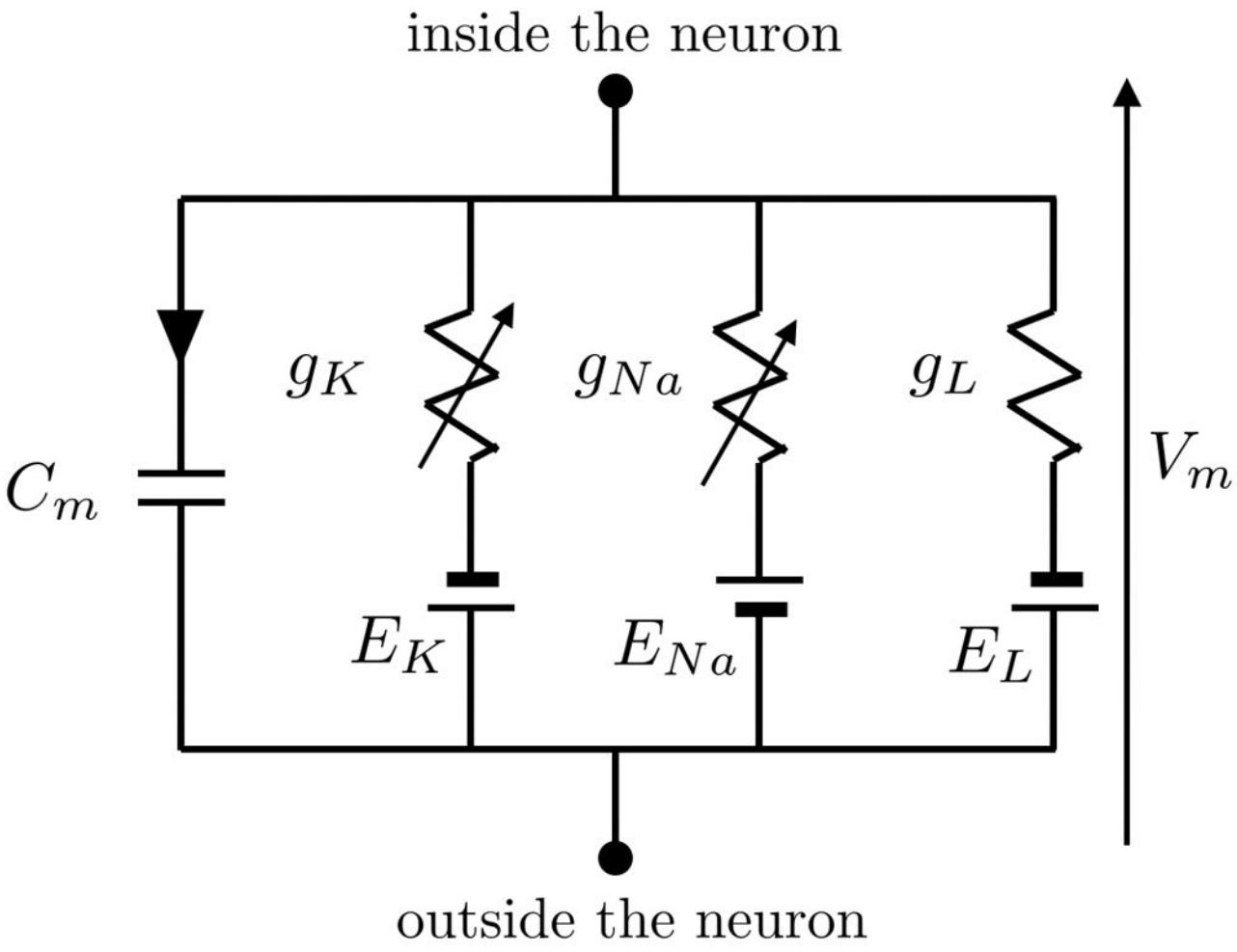

Figure 3.
Electrical equivalent circuit model of neuron with sodium (*Na*) and potassium (*K*) ion-channels and leakage current (*L*).

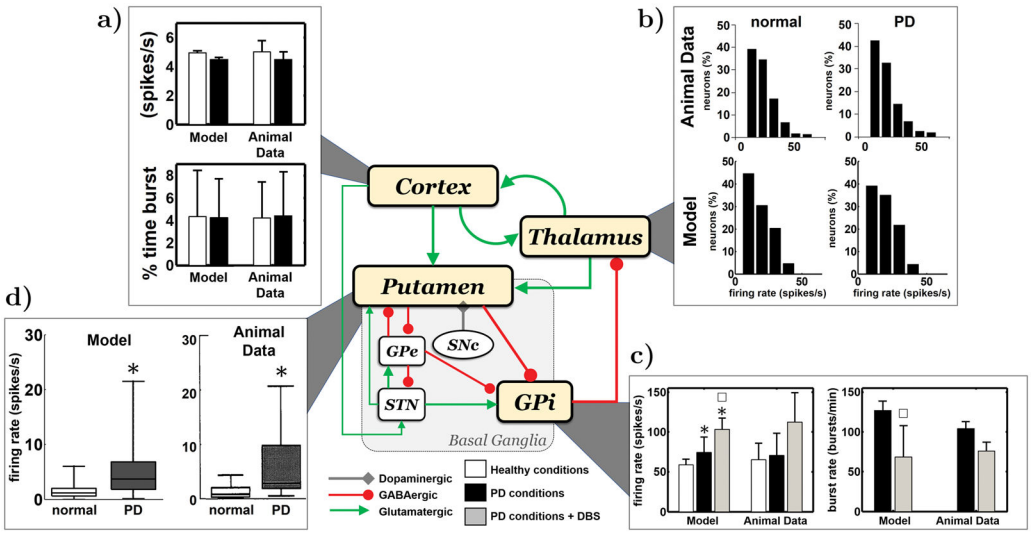

Figure 4.

Example of single-compartment network model of the motor circuit from [58]. a–d) Statistical features of the simulated spike trains are compared to those of single unit spike trains collected in animal models of PD *in vivo* both before and after inducing parkinsonian motor symptoms. Data refers to motor cortex (a), ventrolateral thalamus (b), GPi (c), and putamen (d), respectively. Numerical simulations were designed to mimic the experimental setup used to collect the data. Results from numerical simulations were averaged over 600 neuron models per nucleus and closely reproduced the experimental data. Further description of the statistical features, source of the experimental data, and data collection procedures is reported in [58].

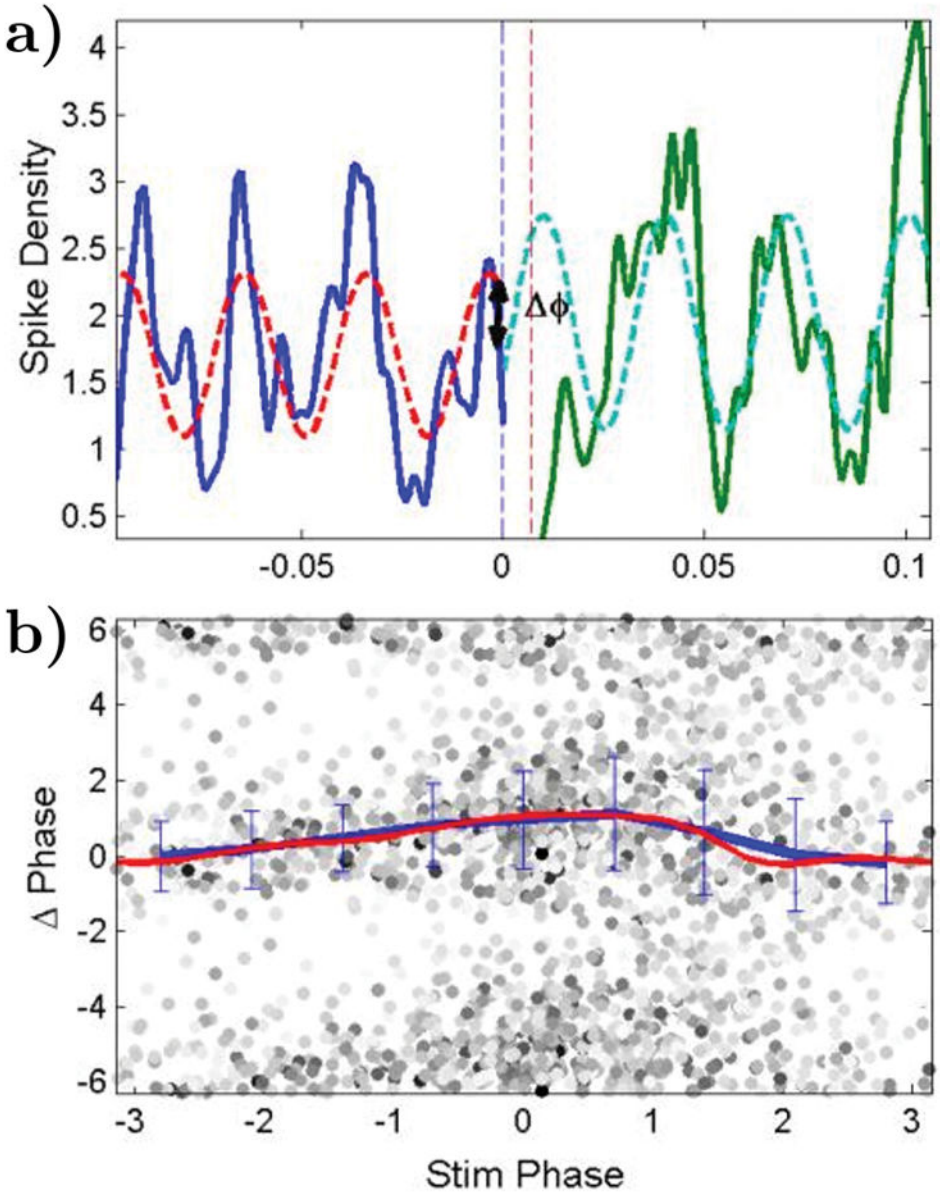

Figure 5.

Example of phase response curve (PRC) estimated from a population of STN neuron models. a) Spike density preceding (solid blue) and following (green) a single DBS pulse. Each spike density is fit separately with a 34 Hz sine wave (dashed lines). b) A plot of the population-average phase change versus the phase at the DBS pulse onset. Gray dots indicate the intensity of neural oscillations in the band 13–30 Hz at the time of each DBS pulse. Figure modified with permission from [83].

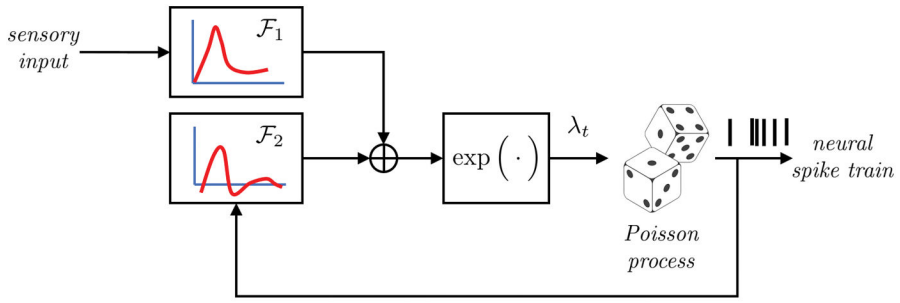

Figure 6.

Schematic of point-process model with a generalized linear structure and dependency of past spiking history and an exogenous sensory stimulus.

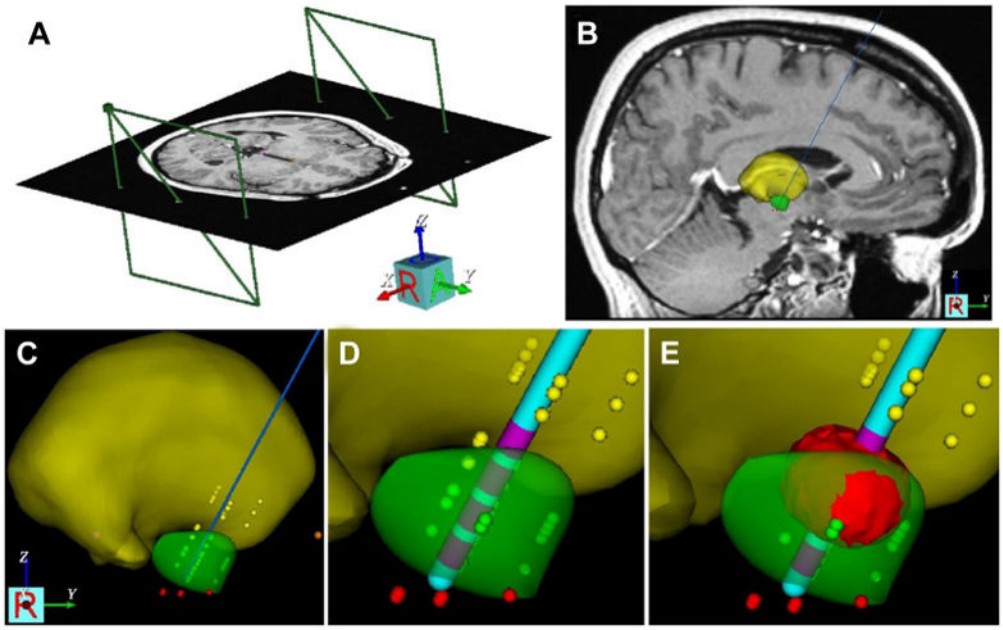

Figure 7.

Example of integration of pre-surgical imaging and multi-compartment modeling to estimate the volume of activated tissue in a PD patient. Solution proposed by McIntyre and colleagues [133]. A–B) Stereotactic coordinate system relative to the patient imaging data (A) and atlas representations of anatomical nuclei. Yellow and green volumes are the thalamus and STN, respectively. The blue line represents the planned surgical trajectory of the DBS electrode. C–D) Stereotactic location (C) and final placement (D) of the DBS electrode, respectively. Yellow, green, and red dots indicate thalamic cells, STN cells, and SNr cells, respectively. Purple cylinders represent the electrode contacts. E) Volume of tissue activated during therapeutic DBS (red volume). Figure reproduced with permission from [133].